RESEARCH PAPER

Synthesis and Characterization of Mercuric Sulfide Nanoparticles Thin Films by Pulsed Laser Ablation (PLA) in Distilled Water (DW)

N. Jassim Mohammed [1,*] and H. Fakher Dagher [2]

** nadheerphys@uomustansiriyah.edu.iq*

Received: January 2020 Revised: March 2020 Accepted: May 2020

[1] Thin Films Laboratory, College of Science, Mustansiriyah University, Baghdad, Iraq.

[2] Research laboratory of Atomic Physics, College of Science, Mustansiriyah University, Baghdad, Iraq.

DOI: 10.22068/ijmse.17.3.11

Abstract: *Thin films of meta-cinnabar mercuric sulfide (β-HgS) nanoparticles (NPs) was prepared by pulsed laser ablation (PLA) utilizing a pellet of cinnabar mercuric sulfide (α-HgS) was immersed in distilled water (DW). Q-switched Nd:YAG laser of 1064 nm wavelengths with repetition rate (1 Hz) and fluency (1.5 J/cm^2) applied for ablation. Structural, morphological, and particle sizes of the β-HgS NPs are investigated by analyzing XRD, AFM, SEM, and TEM measurements. Their crystal structure is transformed from hexagonal (wurtzite) of the α-HgS target material to cubic (zinc blende) β-HgS NPs. The optical properties of the β-HgS NPs are measured by UV–visible spectrophotometer. The direct bandgap is calculated to be (2.45 eV) of small particles (4-6.2 nm) moreover, the bandgap value of smallest particles (1-4 nm) is (3.47 eV) according to the optical transmission spectra.*

Keywords: *Pulsed laser ablation, Nanocrystalline, Mercury sulfide, Cinnabar, Metacinnabar.*

1. INTRODUCTION

Mercuric sulfide (HgS) is one of the most important II-VI semiconductor compounds possessing excellent optoelectronic properties. By using this material in ultrasonic transducers, electrostatic image materials, photoelectric conversion image materials, and photoelectric conversion devices make it important and interesting [1]. HgS has more attention due to their applications as acoustic optical materials [2] and infrared sensing [3]. Generally, the bulk of mercury sulfide consists of cinnabar (hexagonal, red α -HgS) and meta-cinnabar (cubic, black β -HgS) [4, 5]. Cinnabar (α-HgS) is a wide bandgap semiconductor (Eg = 2.0 eV), but it converts to a zinc blend modification (β-HgS) with temperatures above 344 ˚C and becomes a narrow bandgap semi-metal (Eg = 0.5 eV) [6]. As particle sizes decrease to a nanometer scale, quantum confinement effects and large surface to volume ratios make these applications even more significant. In particular, nano-sized HgS has potential use in solid-state solar cells and photoelectrochemical cells [7]. Practical and facile methods to synthesize nano-sized β-HgS particles remain a challenge. Established methods include chemical deposition [8], solvothermal [9] microwave heating [10], photochemical [11], wet chemical [6], and electrochemical [12]. A common difficulty is the aggregation of irregularly shaped particles with a wide size distribution. Particle morphology is difficult to control in methods conducted at ambient temperatures and results in large irregular particles [13].

PLA can be considered as low-cost, facile, and suitable method for the production of nanoparticles for various materials and applications. This technique has been involved in many fields, including bio- applications for the production of nanoparticles as food for some types of bacteria [14] and other physical applications in solar cells to produce nanoparticles in different liquids [15].

In this study, we report a novel method to produce nanoparticles of meta-cinnabar (β-HgS) by phase transformation of cinnabar (α-HgS) powder pressed as pellet and immersed in distilled water. The structural and optical properties of β-HgS nanoparticles produced by laser ablation in distilled water were also investigated.

[DOI: 10.22068/ijmse.17.3.11]

2. EXPERIMENTAL PROCEDURES

The HgS powder employed as pellet with dimensions of 0.7×0.7cm^2 and thickness 0.2cm by pressing under pressure 13 tons and sintering with heating under vacuum at 400 K. Nd: YAG laser employed to ablate a pellet of HgS at the wavelength of (1064 nm) with a repetition rate (1 Hz). The fluency of used laser just after the laser system was (1.5 J/cm^2) and the number shots of laser were 200 pulses. β-HgS thin film was prepared with a thickness of 150 nm. The irradiation laser diameter focused on the mercuric sulfide disc target was 2.0 mm. The shots of laser were focused onto a pellet of HgS semiconductor, which was held inside a quartz vessel involved distilled water with a 1 cm path length (see Fig. 1).

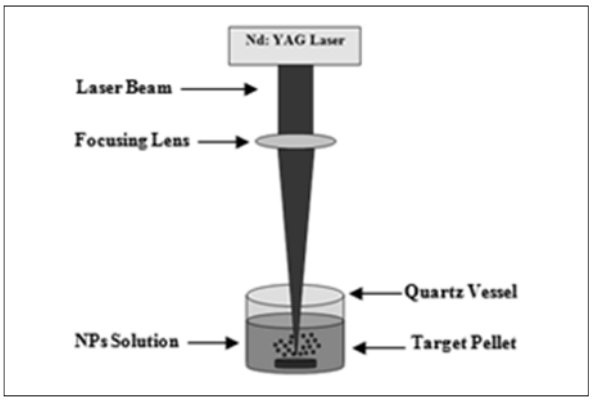

Fig.1. Colloid of β-HgS NPs formation by PLA

The cell sample is placed under the laser beam at a distance of 5 cm with a rotation cell to avoid the drilling effect due to laser ablation. The film of β-HgS NPs was prepared by the preparation of suspension that containing β-HgS NPs produced by PLA on a glass substrate by using drop casting technique at a temperature of up to 65 ˚C as shown in Fig (2).

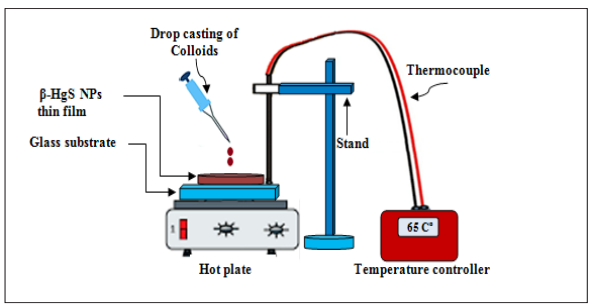

Fig.2. Drop casting method on a glass substrate with a heater of β-HgS colloidal solution.

3. RESULTS AND DISCUSSION

3.1. Structural Studies

HgS target was studied by X-ray diffraction. All the diffraction peaks in the XRD pattern can be indexed to the pure wurtzite structure α-HgS (cinnabar). The peaks correspond to diffraction at 2 theta values of 24.88 related to (100), 26.64 to (101), 28.26 to (003), 31.34 to (102), 37.96 to (103), 43.84 to (110), 44.76 to (111), 45.9 to (104), 47.84 to (112), 51.9 to (201), 52.78 to (113), 54.74 to (105), 58.32 to (006) and 59.2 to (114) planes, which are in good agreement with the JCPDS-pattern (JCPDS No.: 75-1538) for α-HgS as shown in Fig. (3-a).

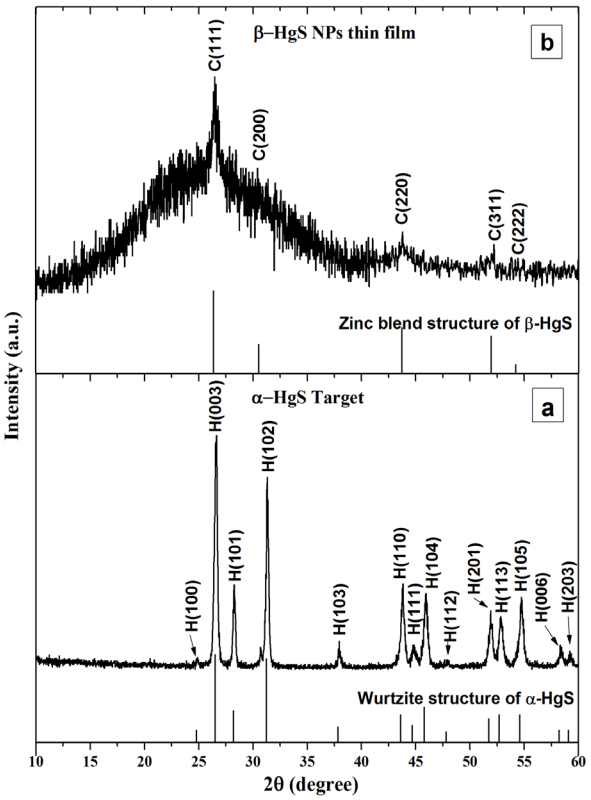

Fig.3. XRD patterns of: a) wurtzite structure of α-HgS target and b) zinc blend of β-HgS NPs thin film.

For zinc blend of β-HgS NPs thin film and amorphous structure with some sharp diffraction, lines have been demonstrated from X-ray investigations by the resulting diffraction pattern. The characteristic zinc blend β-HgS planes of (111), (200), (220), (311) and (222) located at 26.47°, 30.43°, 43.81°, 52.16° and 54.37°, respectively for β HgS NPs thin film

[DOI: 10.22068/ijmse.17.3.11]

in 10-60° 2θ range are observed. All the peeks of the XRD for β HgS thin film in terms of position matched well with those of β HgS zinc blend (JCPDS file No.: 73-1593), as shown in Fig. (3-b).

X-ray investigations were given clearly and through diffraction patterns, there are phase transformations from the wurtzite structure to the zinc blend of HgS, as shown in Fig. (3-a and b).

The crystallite size (d) of the β-HgS NPs thin film was calculated using the Scherrer's equation:

$$d = 0.9\lambda / \beta \cos\theta \qquad (1)$$

where λ = 2.2897 °A is the wavelength of Cu K_ radiation and β is the broadening of the diffraction line measured at half maximum intensity (FWHM).

The crystallite size of the β-HgS NPs has been calculated to be 8.78 nm. The broadening of the peaks indicates that the particles are small in size, as shown in Fig. (3).The formation of nanoparticles of HgS can be observed by microscopic images of SEM. Where many small nanoparticles are observed with the formation of a few particles whose size is relatively larger due to the aggregation of smaller particles due to aging, as shown in Fig. (4).

The presence of mercury (Hg) is evidenced by the predominant peaks of Hg along the EDX spectrum with sulfur (S) and the silicon (Si) produced from the glass substrate. The elemental ratio of Hg to S is 31:27 in the film of β-HgS NPs as shown in Fig. (4).

Fig 5 (a, b, and c) presents two, three dimensional AFM images and the granularity of β-HgS NPs, respectively, where the mean roughness (Ra), mean root roughness (Rq) and the average particle size measurements are 4.77 nm, 5.5 nm,

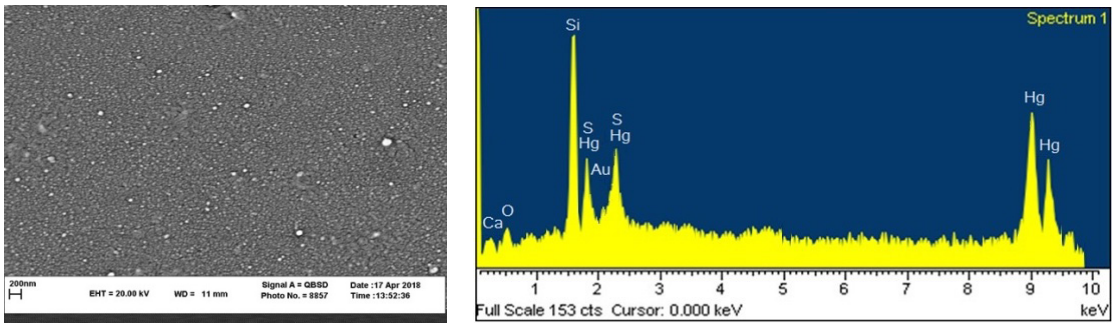

Fig.4. The SEM and EDX images for β-HgS NPs thin film

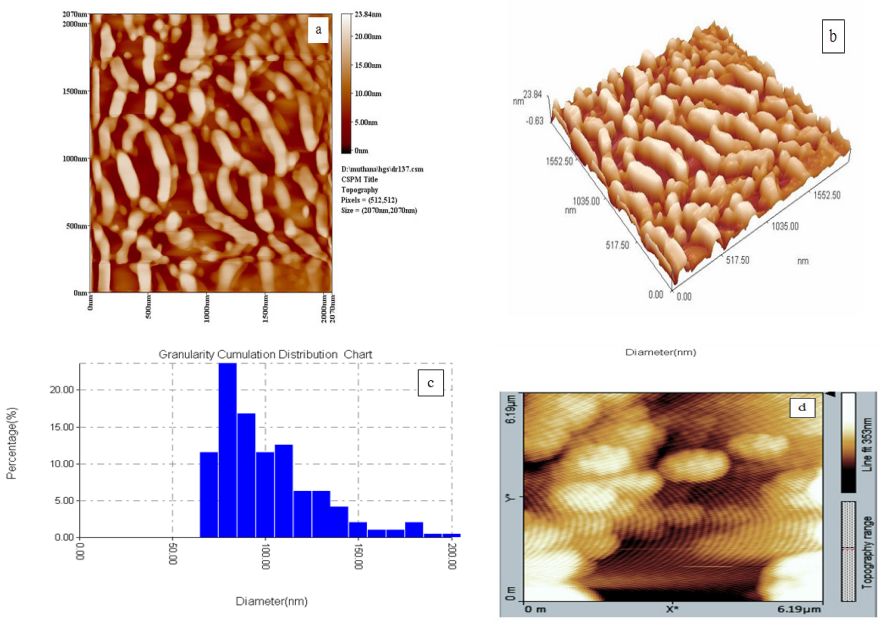

Fig. 5. The AFM images of β-HgS NPs thin film;
a) two-dimensional, b) three-dimensional, c) granularity and d) nanoparticles clusters

[DOI: 10.22068/ijmse.17.3.11]

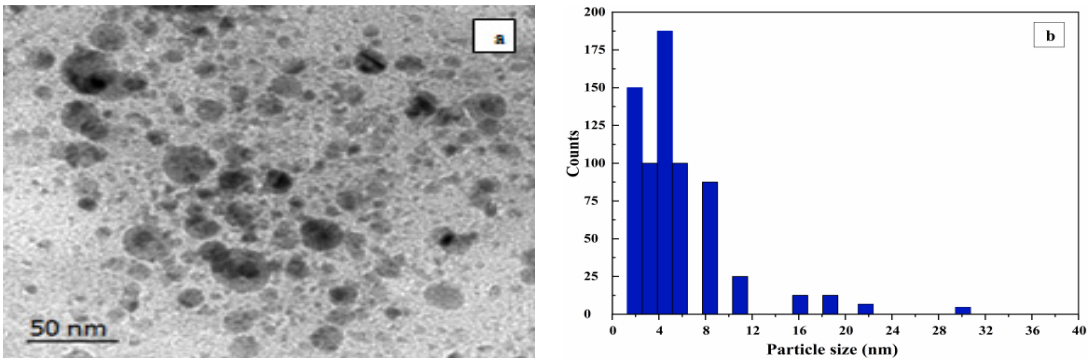

Fig.6. a) TEM image of β-HgS NPs thin film. b) Size distribution of β-HgS NPs thin film calculated based on the TEM image.

and 92 nm, respectively. Also, from the images, several nanoparticle clusters of HgS are formed by the aggregation of small nanoparticles as shown in Fig (5-d).

The preparation of nanoparticles by laser ablation for a target of mercuric sulfide has demonstrated to us the possibility of preparing small nanoparticles with some clusters of these particles due to the aggregation with the aging of the preparation time as observed in the TEM image, as shown in Fig. (6).

As shown in Fig 6-a, the majority of the β-HgS NPs were spherical, well dispersed. Clearly, there are several nanosize that are confirmed by the particle size distribution (Fig. 6-b). The main part of particles has a size less than 31 nm. Their average size is 6 nm.

3.2. Optical Properties

The absorbance spectrum of β-HgS NPs deposited on a glass substrate was measured using a UV-Visible spectrophotometer within the range of 300 to 900 nm. However, it is clear that the absorption edge located at a wavelength of 340 nm, as shown in fig. (7).

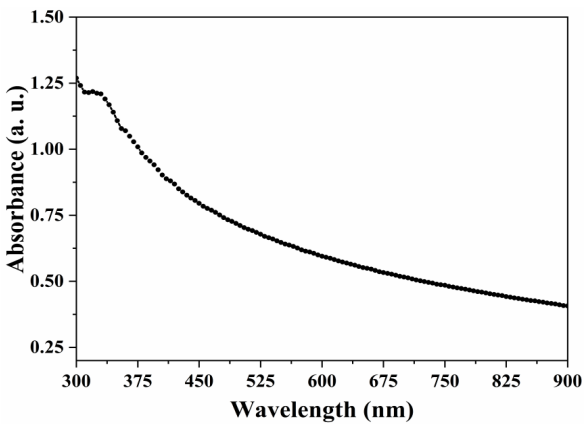

Fig.7. UV-Visible absorbance spectrum of β-HgS NPs thin film

Using the data recorded from the transmittance spectrum of β-HgS NPs thin film, the optical can be calculated at room temperature by using the following equation [16]:

$$(\alpha h\nu)=B(h\nu-E_g)^{(1/2)} \quad (2)$$

where α is the optical absorption coefficient, $h\nu$ is the photon energy, E_g is the optical bandgap, and B is a constant.

An estimate of the optical band-gap is obtained from the extrapolation of the linear plot of $(\alpha h\nu)^2$ vs $(h\nu)$, as shown in fig. (8).

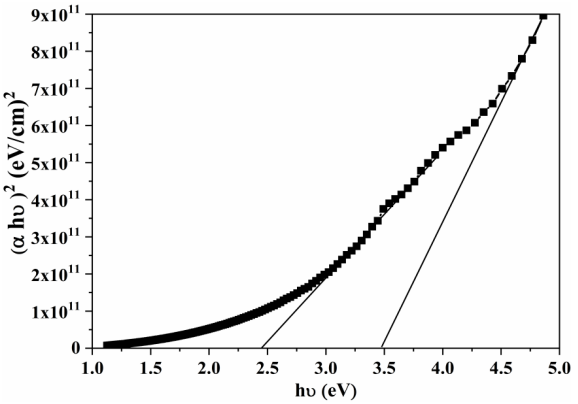

Fig.8. Variations of $(\alpha h\nu)^2$ with $h\nu$ for β-HgS NPs thin film.

It's clear from Fig. 8 that the bandgap value of small particles (4-6.2nm) is 2.45eV. moreover, the bandgap value of the smallest particles (1-4 nm) is 3.47eV, These values of the particle size are equal or less than the Bohr radius of β–HgS NPs (6.2nm) which means the quantum confinement effect is granted [17]. The values of the energy bands for

[DOI: 10.22068/ijmse.17.3.11]

two ranges of the particle size depending on the value of the confinement that occurs of the electrons. Meanwhile, there are still particles larger than Bohr radius (6.2nm) that may have bandgap with blue shift [18], according to the near-field coupling between the particles [19].

All the small and smallest values of the particle size are less than the value of the bulk α -HgS (2.2 eV) [20] due to the formation of small nanoparticles expressed by the size quantization effects. As a result of light absorption, a positive hole generated in the valence band by transferring an electron to the conduction band. The quantization of the energy levels for small particles is a result of the energy difference between the position of the conduction band and a free electron when they are confined to potential wells of small lateral dimension. This effect appears when the size of the particles becomes comparable to the de Broglie wavelength of a charge carrier. The increase in the band-gap of the as-prepared β–HgS NPs is indicative of quantum size effects [21].

4. CONCLUSIONS

As a conclusion to present work, we have succeeded in a simple and facile procedure to prepare the meta-cinnabar phase of mercuric sulfide (β-HgS) by applying pulsed laser ablation on a pellet of α-HgS stilled in distilled water. The method of laser ablation on the target immersed in distilled water improved the preparation conditions and obtained small nanoparticles up to 8 nm and forming clusters of β-HgS NPs in the cubic phase without the toxic chemicals. Phase transformations and the production of small nanoparticles, this technique leads blue-shifted in the bandgap compared with the bulk of HgS.

ACKNOWLEDGMENTS

This work was done with the possibilities available in the thin film laboratory of the Physics Department at the Faculty of Science, University of Mustansiriya/ Iraq / Baghdad.

REFERENCES

1. Zhang, L., Yang, G., He, G., Wang, L., Liu, Q., Zhang, Q., Qin, D., "Synthesis of HgS nanocrystals in the Lysozyme aqueous solution through the biomimetic method." Appl. Surf. Sci., 2012, 258, 8185–8191.
2. Sapriel, J., "Cinnabar (α HgS), a promising acousto optical material." Appl. Phys. Lett., 1971, 19, 533-535.
3. Higginson, K. A., Kuno, M., Bonevich, J., Qadri, S. B., Yousuf, M., Mattoussi, H., "Synthesis and Characterization of Colloidal β-HgS Quantum Dots." J. Phys. Chem., 2002, 106, 9982-9985.
4. Biering, S., Hermann, A., Furthmuller, J., Schwerdtfeger, P., " The unusual solid-state structure of mercury oxide: relativistic density functional calculations for the group 12 oxides ZnO, CdO, and HgO." J. Phys. Chem., 2009, 113, 12427-12432.
5. Biering, S., Schwerdtfeger, P., " A comparative density functional study of the low-pressure phases of solid ZnX, CdX, and HgX: trends and relativistic effects." J. Chem. Phys., 2012, 136, 034504.
6. Mahapatra, A., K., Dash, A., K., "alpha−HgS Nanocrystals: synthesis, structure and optical properties.," Physica, 2006, 35, 9-15.
7. Roberts, G. G., Lind, E. L., Davis, E. A., "Photoelectronic Properties of Synthetic Mercury Sulphide." Crystals. J. Phys. Chem. Solids, 1969, 30, 833-844.
8. Kale, S. S., Lokhande, C. D., "Preparation and Characterization of HgS Films by Chemical Deposition." Mater. Chem. Phys., 1999, 59, 242-246.
9. Qin, A., Fang, Y., Zhao, W., Liu, H., Su, C., "Directionally Dendritic Growth of Metal Chalcogenide Crystals via Mild Template-free Solvothermal Method." J. Cryst. Growth., 2005, 283, 230-241.
10. Ding, T., Zhu, J., "Microwave Heating Synthesis of HgS and PbS Nanocrystals in Ethanol Solvent." Mater. Sci. Eng., 2003, 100, 307-313.
11. Ren, T., Xu, S., Zhao, W., Zhu, J., "A Surfactant-Assisted Photochemical Route to Single Crystalline HgS Nanotubes." J. Photochem. Photobiol., 2005, 173, 93- 98.
12. Patel, B. K., Rath, S., Sarangi, S. N., Sahu, S. N., "HgS Nanoparticles: Structure and Optical Properties." Appl. Phys., 2007, 86, 447-450.
13. Xin, X., Elizabeth, R., Carraway, "Sonication-assisted synthesis of β-mercuric sulfide nanoparticles." Nanomaterials and Nanotechnology, 2012, 2, 2-17.
14. Muslim, S. N., Dham, Z. A., Mohammed, N. J., "Synthesis and characterization of nanoparticles conjugated tannase and using it for enhancement of the antibacterial activity of tannase produced by Serratia marcescens. "Microbial pathogenesis, 2017, 110, 484-493.
15. Agool, I. R., Mohammed, N. J., and Al-Ameer, H. M. A., "Synthesis and Characterization of CdTe

[DOI: 10.22068/ijmse.17.3.11]

NPs Induced by Laser Ablation in Liquids." J. Adv. Phys., 2017, 6, 241-247.
16. Yang, F. F., Fang, L., Zhang, S. F., Liao, K. J., Liu, G. B., Dong, J. X., Li, L. Fu, G. Z., "Optical properties of CdIn2O4 thin films prepared by DC reactive magnetron sputtering." J. Cryst. Growth, 2006, 297, 411-418.
17. Svane, A., et al. "Quasiparticle band structures of β-HgS, HgSe, and HgTe." Physical Review B 84.20, 2011, 205205.
18. Massé, G., J-P. Aicardi, and C. Butti. "Study of band-gap shrinkage in cinnabar (α-HgS) by cathodoluminescence under very strong excitation." physica status solidi (a) 42.2, 1977, 545-552.
19. Al-Haddad, A., et al. "Highly-Ordered 3D Vertical Resistive Switching Memory Arrays with Ultralow Power Consumption and Ultrahigh Density." ACS applied materials & interfaces 8.35, 2016, 23348-23355.
20. Roth, W. L., Physics and Chemistry of II-VI Compounds, (Eds.), Aven, M. Prener, J. S., North-Holland, Amsterdam, 1967, 118.
21. Yang, J. P., Meldrum, F. C., Fendler, J. H., "Epitaxial-Growth of Size-Quantized Cadmium-Sulfide Crystals Under Arachidic Monolayers." J. Phys. Chem., 1995, 99, 5500-5504.

[DOI: 10.22068/ijmse.17.3.11]